Exploring the mechanisms of baicalin in diabetic cardiomyopathy: Insights from network pharmacology and experimental validation

XUYONG ZHAO, LINA XIE and NING ZHU

Department of Cardiology, The Wenzhou Third Clinical Institute Affiliated to Wenzhou Medical University, Wenzhou People's Hospital, Wenzhou, Zhejiang 32500, P.R. China

Received January 14, 2026; Accepted April 29, 2026

DOI: 10.3892/br.2026.2170

Abstract. Baicalin has protective effects against a range of cardiovascular conditions, such as myocardial ischemia-reperfusion injury, cardiac dysfunction, and apoptosis in cardiomyocytes. However, the underlying protective mechanisms in diabetic cardiomyopathy (DCM) remain unclear. The present study aimed to investigate the specific molecular mechanism activated by baicalin to ameliorate DCM. The effects of baicalin were investigated *in vitro* and its potential targets and pathways were identified using network pharmacology, molecular docking, echocardiography, reverse transcription PCR, ELISA, histopathology, immunofluorescence staining and western blotting. Baicalin significantly alleviated high-glucose (HG)-induced injury in H9c2 cells by inhibiting fibrotic markers, inflammatory factors and pyroptosis. Moreover, protein tyrosine phosphatase non-receptor type 22 (PTPN22) and tumor necrosis factor (TNF) were identified as crucial targets for baicalin. Molecular docking indicated that baicalin exhibited a strong binding affinity for PTPN22 and TNF. Baicalin successfully suppressed HG-induced pyroptosis, inflammation and fibrotic markers in addition to inhibiting the activation of TNF-α and PTPN22 signaling pathways. In addition, PTPN22-small interfering RNA treatment modulated pyroptosis *in vitro*. The present study offers insight into the key therapeutic mechanisms activated by baicalin, and its potential therapeutic targets, PTPN22 and TNF-α.

Introduction

Diabetic cardiomyopathy (DCM) is a distinct, chronic complication of diabetes, particularly in patients with long-standing, poorly controlled hyperglycemia, and is a notable cause of heart failure and cardiovascular disease (CVD), characterized by pathological changes of the cardiac structure and function. It occurs independently of other cardiovascular risk factors, such as hypertension or coronary artery disease (1)[1] and contributes to CVD-induced mortality and morbidity in diabetic patients (2). During the early stages of CVD, increased lipid metabolism and impaired glucose metabolism are initiated, which induce excessive oxidative stress and inflammation. Excessive reactive oxygen species production and the activation of excessive oxidative stress and inflammation lead to myocardial damage and remodeling, typically impairing the diastolic function first. With the progression of the disease, systolic dysfunction develops and heart failure occurs (3).

Scutellaria baicalensis Georgi, particularly its primary active flavonoid, baicalin, offers therapeutic effects against cardiotoxicity (4), myocardial ischemia (5), obesity-induced cardiac dysfunction (6) and autoimmune myocarditis (7)- and doxorubicin-induced cardiotoxicity (8). *S. baicalensis* can treat CVD by specifically inhibiting apoptosis, decreasing oxidative stress and inflammation and preventing cardiac fibrosis (9-11). It targets pro-inflammatory markers (TNF-α, IL-6, IL-1β and IL-8) while increasing the levels of the anti-inflammatory cytokines (IL-10) in myocardial tissues, which results in improved cardiac function (12). Baicalin protects against DCM by acting on multiple, complex and interrelated pathways rather than a single target (13,14). Therefore, key pathways and therapeutic targets involved in its mechanism of action require a more comprehensive investigation and further exploration.

Network pharmacology is an accessible method for systematically identifying multi-target and -pathway mechanisms of drug action and is used in numerous studies to determine active compounds and underlying mechanisms (15,16). It enables the identification of potential drug-target-disease interactions, facilitating the exploration of novel therapeutic applications. The present study employed the network pharmacology approach to evaluate the therapeutic action of baicalin on DCM, focusing on the interactions between candidate drug- and disease-related targets (17). Furthermore, the potential molecular mechanism of action underlying the protective effects of baicalin on DCM was explored using network pharmacology and *in vitro* assessments.

Correspondence to: Dr Ning Zhu, Department of Cardiology, The Wenzhou Third Clinical Institute Affiliated to Wenzhou Medical University, Wenzhou People's Hospital, 299 Guan Road, Wenzhou, Zhejiang 32500, P.R. China
E-mail: zhuningccc@126.com

Key words: baicalin, diabetic cardiomyopathy, network pharmacology, experimental validation

Materials and methods

Common target of baicalin and DCM prediction. Swiss target prediction (swisstargetprediction.ch/) was used to discover potential targets for baicalin. The candidate genes of DCM were screened from the Comparative Toxicogenomics Database (ctdbase.org) and the GeneCards database (genecards.org/). The threshold for inclusion was set at an inference score >30. Duplicate targets were eliminated, and the shared targets were entered into the Venny diagram 2.1 online platform (bioinfogp.cnb.csic.es/tools/venny/index.html.) to visualize the overlapping targets. Potential candidate targets were imported into the WebGestalt server (version 2024; webgestalt.org/) for Gene Ontology (GO) (18) and Kyoto Encyclopedia of Genes and Genomes (KEGG) enrichment analyses (kegg.jp/KEGG).

Molecular docking. Molecular docking analysis was performed as previously described (19). The 2D chemical structure of baicalin was retrieved from the PubChem (pubchem.ncbi.nlm.nih.gov) database and prepared for molecular docking by adding hydrogen atoms, followed by free energy minimization using the CB-Dock2 platform (2022; cadd.labshare.cn/cb-dock2/php/index.php). The crystal structures of protein tyrosine phosphatase non-receptor type 22 (PTPN22) and tumor necrosis factor (TNF)-α were retrieved from the Protein Databank (rcsb.org/) and modified by adding hydrogen atoms and eliminating water molecules. The CB-Dock2 platform was used to calculate the binding affinity energy. PyMol software (version 2.6; pymol.org/) and BIOVIA Discovery Studio Visualizer (version 2021; discover.3ds.com/discovery-studio-visualizer-download) were used to visualize the interactions between the ligand and receptor molecules.

Culture of H9c2 cardiomyocyte cells and small interfering (si)RNA transfection. H9c2 (Cellverse Co., Ltd.) cells were cultured in DMEM (HyClone; Cytiva) with 10% fetal bovine serum (Sigma-Aldrich; Merck KGaA) and 1% penicillin-streptomycin and were maintained at 37˚C in a 5% CO_2 environment. The cells were grouped as follows: Control (5.5 mM glucose), high-glucose (HG; 33 mM glucose), HG + with low-dose baicalin (50 μM; HG + BL), HG + high-dose baicalin (100 μM; HG + BH) and HG + PTPN22-siRNA. All treatment was performed at 37˚C for 24 h. Cells were transfected with siRNA (Shanghai GenePharma Co., Ltd) once they reached a confluence of 60-80%. Lipo3000-B reagent was diluted with Opti-MEM (Gibco; Thermo Fisher Scientific, Inc.) and mixed thoroughly. siRNA (Table SI) was diluted to 50 nM with Opti-MEM. Lipo3000-A reagent (Invitrogen; Thermo Fisher Scientific, Inc.; cat. no. L3000001) and Lipo3000-B reagent were added at room temperature for 5-15 min. The contents of the tubes were added to the cells. The cell culture medium was replaced with normal medium for subsequent experiments 6 h after transfection. The samples were collected 48 h later for subsequent experimental detection.

Cell viability. Cell viability was detected using Cell Counting Kit-8 (Abbkine Scientific Co., Ltd.), according to the manufacturer's instructions. After being exposed to baicalin (50 or 100 μM) for 48 h at 37˚C, CCK-8 solution was added for 1 h at 37˚C. The absorbance of the resulting solution was evaluated with a microplate reader at a wavelength of 450 nm.

Calcein-AM staining. Staining of cells was performed according to the manufacturer's instructions of the Calcein-AM staining kit (Beyotime) at 37˚C in the dark for 30 min. After incubation, fluorescence can be directly detected using a fluorescence microplate reader (excitation wavelength: 494 nm, emission wavelength: 517 nm).

Reverse transcription-quantitative (RT-q)PCR. Total RNA was extracted from cells using the Total RNA Isolation Kit (cat. no. RE-030111, Fuji) according to the manufacturer's instructions. Total RNA were reverse-transcribed into complementary DNA using the 1st Strand cDNA Synthesis Kit (cat. no. KY01, KeyCloud Biotech), according to the manufacturer's protocol. RT-qPCR was performed on an ABI QuantStudio™ 12 K Flex real-time PCR system (Applied Biosystems; Thermo Fisher Scientific, Inc., Waltham, MA, USA) using the 2x SYBR Green qPCR Master Mix (cat. no. KY02, KeyCloud Biotech, China). The primer sequences for collagen I, transforming growth factor-β1 (TGF-β1), connective tissue growth factor (CTGF), C-C motif chemokine ligand 20 (CCL20), colony-stimulating factor 1 (CSF1), CSF2, and the housekeeping gene glyceraldehyde-3-phosphate dehydrogenase (GAPDH) are listed in Table SII. Thermocycling conditions were as follows: initial denaturation at 95˚C for 30 sec, followed by 40 cycles of denaturation at 95˚C for 5 sec and combined annealing/extension at 60˚C for 30 sec. Relative mRNA expression levels were quantified using the 2-ΔΔCq method with GAPDH as the endogenous reference gene (20). All target gene expression levels were normalized to the average value of the control group.

Apoptosis analysis. Cell apoptosis was assessed using the TUNEL assay kit (cat. no. KTA2011; Abbkine Scientific Co., Ltd.) according to the manufacturer's instructions. Cells were fixed with 4% paraformaldehyde at room temperature for 30 min and rinsed with PBS for 5 min, followed by permeabilization using 0.02 μg/μl proteinase K. TUNEL detection solution was then applied for 10 min at room temperature. slides were washed by PBS at room temperature twice for 5 min each time. Nuclei were stained with 0.05 μg/μl DAPI solution at room temperature for 10 min in the dark. Mounting medium was antifade mounting medium (Beijing Solarbio Science & Technology Co., Ltd.). A fluorescence microscope was used to determine the proportion of TUNEL-positive cells (UltraVIEW VoX & IX81, Olympus Corporation). 3 fields of view were randomly selected in each group.

Immunofluorescence staining analysis. Cells were fixed with 4% paraformaldehyde at room temperature for 15 min. Heat-induced antigen retrieval at 100˚C was performed, followed by washing with PBS (pH 7.4). The slices were treated with 3% BSA (Sigma) at room temperature for 2 h and incubated with primary antibody (GSDMD-N, Proteintech, cat. No 66387-1-Ig, 1:200) overnight at 4˚C and FITC-labeled goat anti-mouse IgG (1:10,000; cat.no A0568; Beyotime Biotechnology) for 1 h at room temperature. DAPI

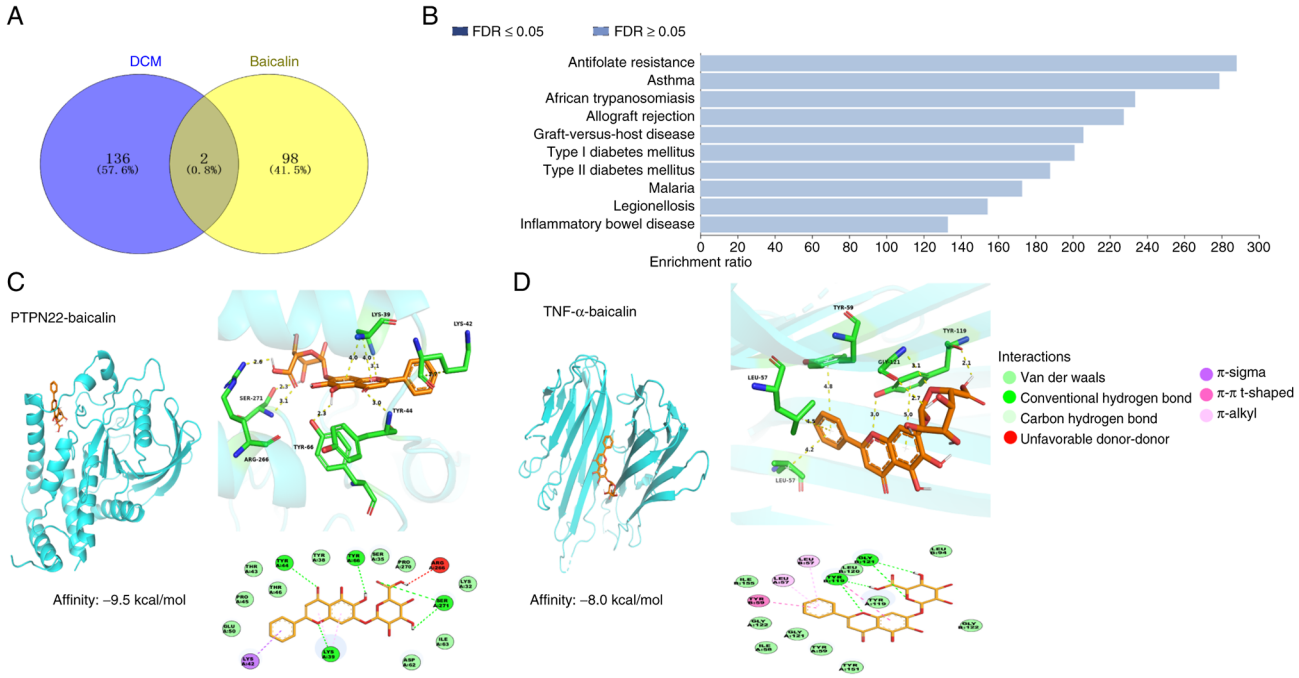

Figure 1. Network pharmacology and molecular docking analysis of the mechanisms of baicalin in the treatment of DCM. (A) Venn diagram showing the key targets of baicalin in DCM treatment. (B) Kyoto Encyclopedia of Genes and Genomes enrichment analysis of signaling pathways involved. Molecular docking analysis of the binding sites between baicalin and (C) PTPN22 and (D) TNF-α. DCM, diabetic cardiomyopathy; PTPN, protein tyrosine phosphatase non-receptor type; FDR, false-discovery rate.

was added in the dark at room temperature for 5 min. Images were captured by a Nikon fluorescence microscope (NIKON ECLIPSE TI-SR, Nikon Corporation). Image analysis was performed using ImageJ software (version 1.54k, National Institutes of Health).

Western blotting. Protein was extracted from cells using RIPA lysis buffer (cat. no. BL504A; Biosharp) supplemented with phosphatase and protease inhibitors. The protein concentrations in the supernatants were assessed by the BCA Protein Assay kit (Beyotime Biotechnology). Equal amounts of proteins (50 μg/lane) were separated using 10-12% SDS-PAGE, transferred to a PVDF membrane, blocked with 5% BSA (Sigma-Aldrich; Merck KGaA) at room temperature for 2 h and then incubated with primary antibodies as follows: CTGF (cat. no. 25474-1-AP; 1:2,000), collagen I (cat. no. 67288-1-Ig; 1:1,000), TGF-β (cat. no. 21898-1-AP; all Proteintech Group, Inc.; 1:2,000), GSDMD (gasdermin D)-N (cat. no. bs-14287R; BIOSS), PTPN22 (cat. no. 11783-1-AP; both 1:1,000), apoptosis-associated speck-like protein containing a CARD (ASC; cat. no. 10500-1-AP; both Proteintech Group, Inc.; 1:20,000), NLRP3 (cat. no. ab263899; Abcam), Caspase-1 (cat. no. AF5418; Affinity Biosciences; both 1:1,000), IL-1β (cat. no. 16806-1-AP; 1:5,000), IL-18 (cat. no. 10663-1-AP; 1:10,000), TNFα (cat. no. 17590-1-AP; 1:1,000), phosphorylated (p-)p38, p38 (cat. no. 28796-1-AP and 66234-1-Ig; both 1:3,000), p-ERK, ERK (cat. nos. 28733-1-AP and 16443-1-AP; all Proteintech Group, Inc.; both 1:2,000), p-JNK, JNK (cat. no. ABP50351and ABP51663; both Abbkine Scientific Co., Ltd.; both 1:1,000) and GAPDH (cat. no. 60004-1-Ig; Proteintech Group, Inc.; 1:50,000) at 4˚C with gentle shaking overnight. Immunoreactive bands were revealed by HRP-conjugated anti-rabbit or anti-mouse IgG (Beyotime Biotechnology; cat. no. A0208 and A0216; 1:1,000) for 1h at room temperature. Protein bands were visualized with an enhanced chemiluminescence (ECL) kit (Abbkine). Protein bands were detected and analyzed by fully automatic chemiluminescence imaging system (5200Multi, Tanon). Densitometry was analyzed by Tanon GIS 1D (version 4.2; 5200Multi, Tanon).

Statistical analysis. All data are presented as the mean ± standard deviation of three independent experimental repeats and were analyzed with GraphPad Prism 9.5 (Dotmatics). Data were analyzed by one-way ANOVA followed by Tukey's post hoc test. $P<0.05$ was considered to indicate a statistically significant difference.

Results

Potential targets of baicalin against DCM. A total of 138 common targets associated with DCM and 100 targets associated with baicalin were identified (Table SIII). PTPN22 and TNF were shared targets between baicalin and DCM (Fig. 1A). KEGG) analysis did not identify any significant pathways associated with the effects of baicalin on DCM (Fig. 1B).

Molecular docking. Baicalin exhibited a binding affinity of -9.5 kcal/mol for PTPN22 (Fig. 1C). Based on 3D and 2D interaction analysis, baicalin had a strong affinity for PTPN22, with key residues GLU50, PRO45, THR43, THR46, TYR38, SER35, PRO270, LYS32, ILE63 and ASP62 facilitating stabilization primarily through van der Waals interactions. Additionally, baicalin formed stable hydrogen

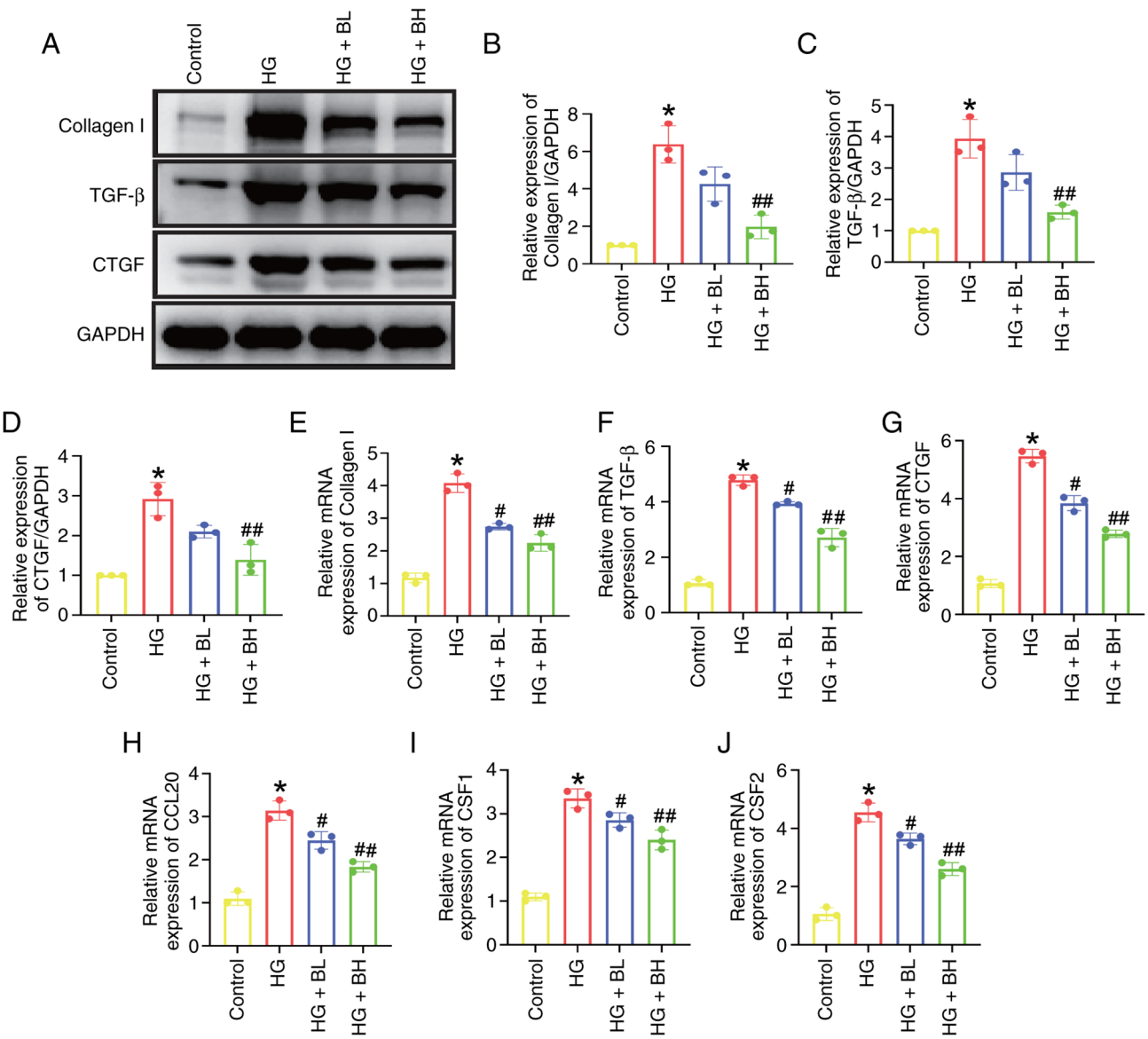

Figure 2. Baicalin suppresses HG-induced release of fibrotic and inflammatory markers in H9c2 cells. (A) Western blotting analysis of (B) collagen I, (C) TGF-β and (D) CTGF protein expression in H9c2 cells challenged with HG (33 mM glucose) in the presence or absence of baicalin (BL: 50 μmol; BH: 100 μmol) for 24 h. Quantitative analysis of (E) collagen I, (F) TGF-β, (G) CTGF, (H) CCL20, (I) CSF1 and (J) CSF2 mRNA levels detected by reverse transcription-quantitative PCR. *P<0.05 vs. Control; $^{\#}$P<0.05, $^{\#\#}$P<0.05 vs. HG. HG, high-glucose; CTGF, connective tissue growth factor; BL, baicalin low; BH, baicalin high; CCL, C-C motif chemokine ligand; CSF, colony stimulating factor.

bonds with TYR44, TYR66, SER271 and LYS39. The stable binding of baicalin to PTPN22 involved π-alkyl interactions with LYS39 and π-sigma interactions with LYS42. However, an unfavorable donor-donor interaction was found with the ARG266 residue. Baicalin demonstrated a binding affinity of -8.0 kcal/mol for TNF (PDB ID: 5MU8; Fig. 1D). The 3D and 2D interaction maps indicated that baicalin bound TNF primarily through van der Waals interactions, with key residues including TYR151, TYR59, GLY121, ILE58, GLY122, ILE155, LEU120, TYR119, LEU94 and GLY122 forming the binding pocket. The stable binding of baicalin to TNF was achieved through hydrogen bonds with TYR119 and GLY121. Additionally, the stable binding involved π-alkyl interactions with the residues LEU57 and LEU57. Finally, baicalin interacted with TNF through π-π T-shaped interactions with the TYR59 and TYR119 residues.

Baicalin suppresses the secretion of HG-induced fibrotic and inflammatory markers in vitro. Western blot and RT-qPCR analyses of H9c2 cell lysates demonstrated that HG significantly elevated the expression levels of fibrotic markers, such as collagen I, TGF-β and CTGF (Fig. 2A-G), as well as inflammatory markers, including CCL20, CSF1, and CSF2 (Fig. 2H-J). However, BH significantly counteracted these changes compared with HG group.

Baicalin mitigates HG-induced pyroptosis in vitro. Fig. 3A displays HG-induced characteristic morphological changes in H9c2 cells, including swelling and rupture of the cell membrane. Calcein-AM staining revealed increased membrane damage resulting from HG exposure (Fig. 3B and H). CCK-8 assay showed that baicalin protected H9c2 cells against HG-induced cell death (Fig. 3G), a finding corroborated by TUNEL

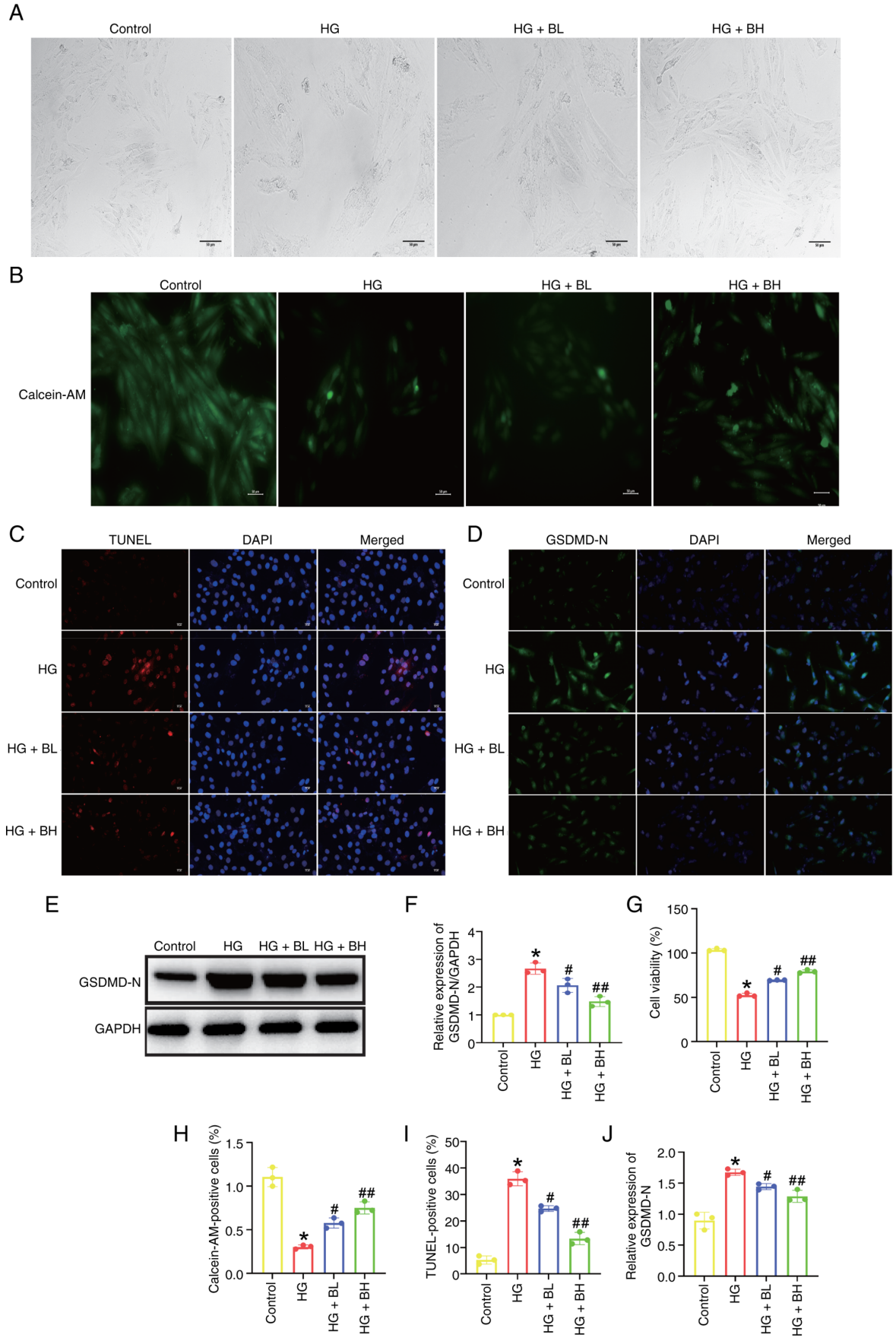

Figure 3. Baicalin mitigates HG-induced pyroptosis in H9c2 cells. (A) Morphological changes of H9c2 cells treated with HG or baicalin (BL: 50 μmol/l; BH: 100 μmol/l) for 24 h. Scale bar, 50 μm. (B) Calcein-AM, (C) TUNEL and (D) immunofluorescence staining of H9c2 cells. Scale bar, 20 μm. (E) Western blotting of (F) GSDMD-N protein expression. (G) Cell viability detected by Cell Counting Kit-8 assay. Quantitative analysis of (H) Calcein-AM staining, (I) TUNEL-positive cells and (J) GSDMD-N immunofluorescence staining. *P<0.05 vs. Control; $^{\#}$P<0.05, $^{\#\#}$P<0.05 vs. HG. HG, high-glucose; GSDM, gasdermin; BL, baicalin low; BH, baicalin high.

staining (Fig. 3C and I). Additionally, baicalin was found to reduce the expression of the pyroptosis marker-GSDMD-N, increased by exposure to HG (Fig. 3D-F and J).

Baicalin inhibits the activation of the TNF and PTPN22 signaling pathways induced by HG in vitro. The present study aimed to verify the effects of baicalin on the TNF and PTPN22 signaling pathways *in vitro*. BH decreased the elevated TNF-α expression as well as p38, ERK and JNK phosphorylation levels compared with HG (Fig. 4A-E). BH significantly decreased the elevated expression levels associated with the PTPN22 signaling pathway, including PTPN22, NLRP3, ASC, caspase, IL-1β, and IL-18 compared with HG group (Fig. 4F-L).

PTPN22 inhibition attenuated HG-induced pyroptosis in vitro. The role of PTPN22 in HG-induced pyroptosis was investigated by PTPN22-siRNA transfection. The successful knockdown of PTPN22 in cells was confirmed by western blot analysis (Fig. S1). Based on the results, the siRNA PTPN22#2 was selected for subsequent studies. Based on the findings from the morphological analysis (Fig. 5A) and Calcein-AM (Fig. 5B and L) staining, HG-induced cell swelling and membrane rupture were reduced when PTPN22 was silenced. PTPN22-siRNA decreased cell apoptosis (Fig. 5C and M) and the expression of GSDMD-N (Fig. 5D and N). Additionally, PTPN22 inhibition effectively blocked the NLRP3 signaling pathway (Fig. 5E-K).

Discussion

The present study investigated the underlying mechanisms of the protective effects of baicalin against DCM. Using network pharmacology, two important targets linked to baicalin-induced therapeutic effects on DCM were identified, namely, PTPN22 and the TNF-α pathway. The binding interactions of baicalin with PTPN22 and TNF-α were confirmed using molecular docking. Baicalin was shown to protect against HG-induced injury by inhibiting the pyroptosis pathway, decreasing inflammation and mitigating fibrotic responses. It serves as a therapeutic agent by blocking the activation of TNF and PTPN22 pathways. Furthermore, the inhibition of PTPN22 suppresses this detrimental signaling, decreasing HG-induced pyroptosis and cellular damage.

DCM is characterized by structural and functional abnormalities, including inflammation, oxidative stress, cardiac lipotoxicity, mitochondrial dysfunction and endoplasmic reticulum stress (21), which collectively cause cardiomyocyte death and fibrosis. These processes lead to left ventricular remodeling and decreased ejection fraction, typically resulting in severe heart failure and high mortality rates (22). Numerous studies have demonstrated that diabetes mellitus increases both the susceptibility and incidence of heart failure by around 2.5-fold; notably, this figure doubles in female patients, irrespective of age and accompanying conditions such as coronary artery disease and dyslipidemia (23-27). *In vivo* studies have shown baicalin-induced therapeutic effects against DCM, revealing that it improves cardiac function in DCM via the regulation of autophagy (28,29). Baicalin is also reported to treat DCM by reducing activation of the purinergic receptor P2Y, G Protein Coupled 12 receptor and NRF2/P62 *in vivo (*30,31). However, the mechanisms by which baicalin decreases HG-induced damage in H9c2 cells are unknown. The present study demonstrated baicalin decreased pyroptosis and fibrotic and inflammatory markers *in vitro*.

Diabetes is marked by persistent inflammation, which serves a role in the progression of DCM. Elevated levels of inflammatory cytokines, particularly TNF-α, IL-6, and IL-1β, are key drivers of DCM, promoting structural damage through cardiac remodeling and fibrosis (32). TNF initiates the recruitment of receptor-interacting protein kinase 1 and cell division cycle 37 and heat shock protein 90 to form a complex that produces active IKK complexes (33). This activation stimulates the kinases p38, ERK and JNK, ultimately leading to the upregulation of pro-inflammatory genes (34). An increase in genes associated with the TNF signaling pathway, including CCL20, CSF1 and CSF2, has been observed during the inflammatory response (35). By targeting key proteins involved in inflammatory signaling, therapeutic approaches for the treatment of DCM may be established. Here, baicalin showed therapeutic potential in DCM by directly binding and inhibiting TNF-α. It suppressed HG-induced inflammation by downregulating TNF-α expression and inhibiting downstream p38, ERK and JNK phosphorylation. Baicalin also decreased expression of pro-inflammatory factors such as CCL20, CSF1 and CSF2, mitigating HG-induced injury. Therefore, baicalin modulated TNF-α pathways in DCM.

Pyroptosis is a pro-inflammatory form of programmed cell death defined by GSDM-mediated plasma membrane rupture (36). Pyroptosis has been identified as a key factor in DCM (37-39). When activated, NLRP3 oligomers are formed, triggered by stimuli, including microbes, particulate matter and damage-associated molecules. This process facilitates the recruitment of the adaptor protein (ASC) and caspase-1 (40), resulting in the cleavage of GSDMD. Caspase-1 converts pro-IL-1β and pro-IL-18 into their active forms. The N-terminal domain of GSDMD forms pores that cause cell swelling, promoting IL-1β and IL-18 release. Baicalin reduces inflammatory diseases by inhibiting pyroptosis (41). However, its specific role in DCM requires further study. Here, treatment with baicalin *in vitro* alleviated HG-induced pyroptosis. PTPN22 encodes the lymphoid-specific tyrosine phosphatase, a crucial regulator in hematopoietic cells (42). The present study demonstrated that baicalin can bind to PTPN22 and inhibit the HG-induced upregulation of PTPN22 expression. While KEGG analysis did not identify any significant signaling pathways associated with baicalin-induced therapeutic effects on DCM, PTPN22 is involved in controlling the activation of the NLRP3 inflammasome and the IL-1β pathway (43). Moreover, baicalin suppressed the expression of GSDMD, PTPN22, NLRP3, ASC, caspase, IL-1β and IL-18, indicating that PTPN22 may induce DCM via the pyroptosis pathway-PTPN22 inhibition also blocked pyroptosis and the NLRP3 signaling pathway, suggesting PTPN22 regulated pyroptosis via the NLRP3 signaling pathway.

Expression of PTPN22 is inhibited by TNF-α in peripheral blood mononuclear cells (44). PTPN22/22 loss of function increases TNF-α secretions in Jurkat T cells (45). Upregulation of TNF-α is observed in PTPN22 1858C/T single-nucleotide polymorphism in rheumatoid arthritis (46). However, the exact

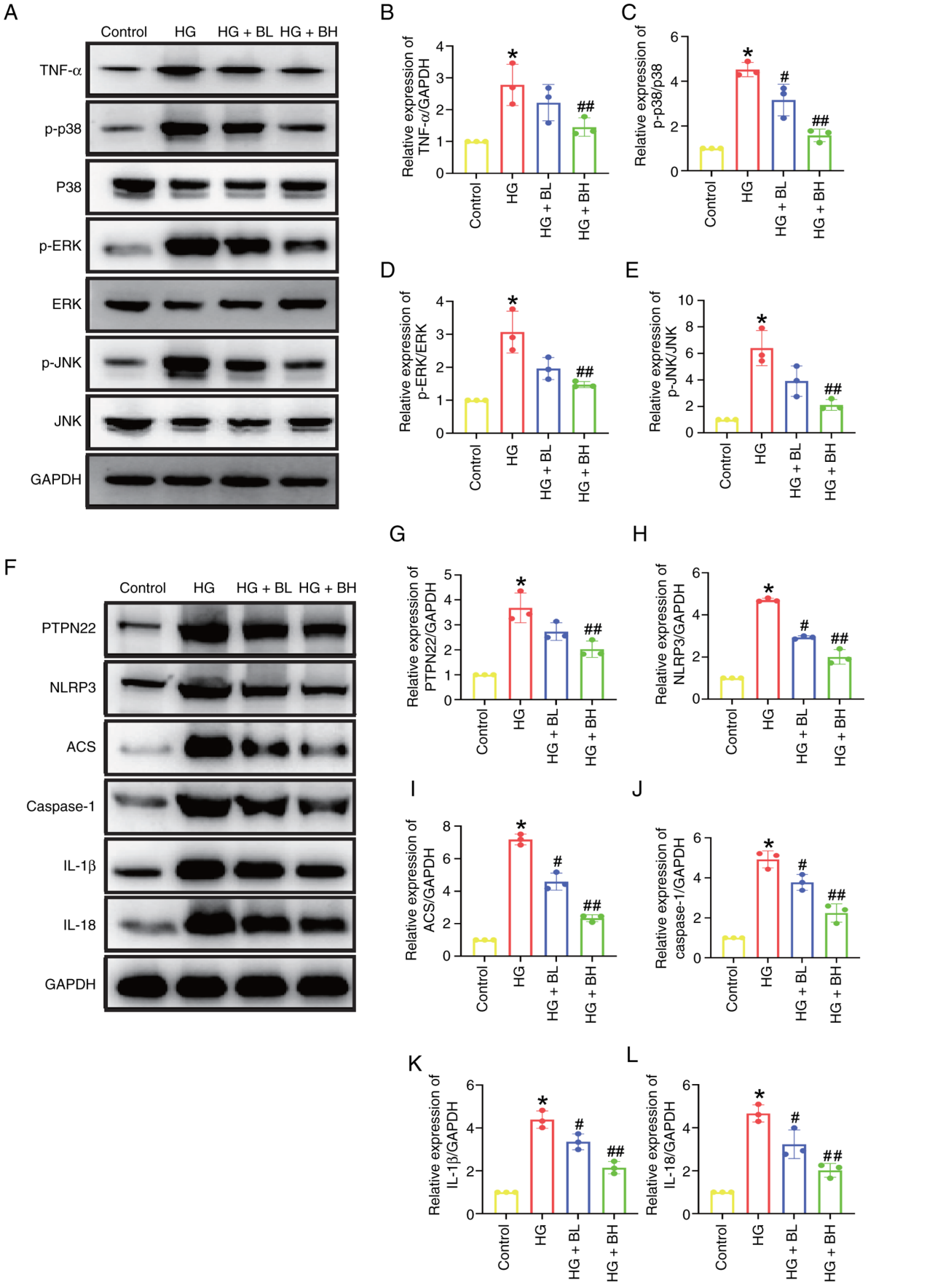

Figure 4. Baicalin inhibits HG-induced activation of TNF and PTPN22 signaling pathways in H9c2 cells. H9c2 cells were treated with HG, or baicalin (BL: 50 μm; BH: 100 μm) for 24 h. (A) Western blotting of (B) TNF-α expression and phosphorylation levels of (C) p38, (D) ERK and (E) JNK. (F) Western blot analysis of (G) PTPN22, (H) NLRP3, (I) ASC, (J) caspase, (K) IL-1β and (L) IL-18 expression. *P<0.05 vs. Control; $^{\#}$P<0.05, $^{\#\#}$P<0.05 vs. HG. HG, high-glucose; BL, baicalin low; BH, baicalin high; p-, phosphorylated; PTPN, protein tyrosine phosphatase non-receptor type; ASC, apoptosis-associated speck-like protein containing a CARD..

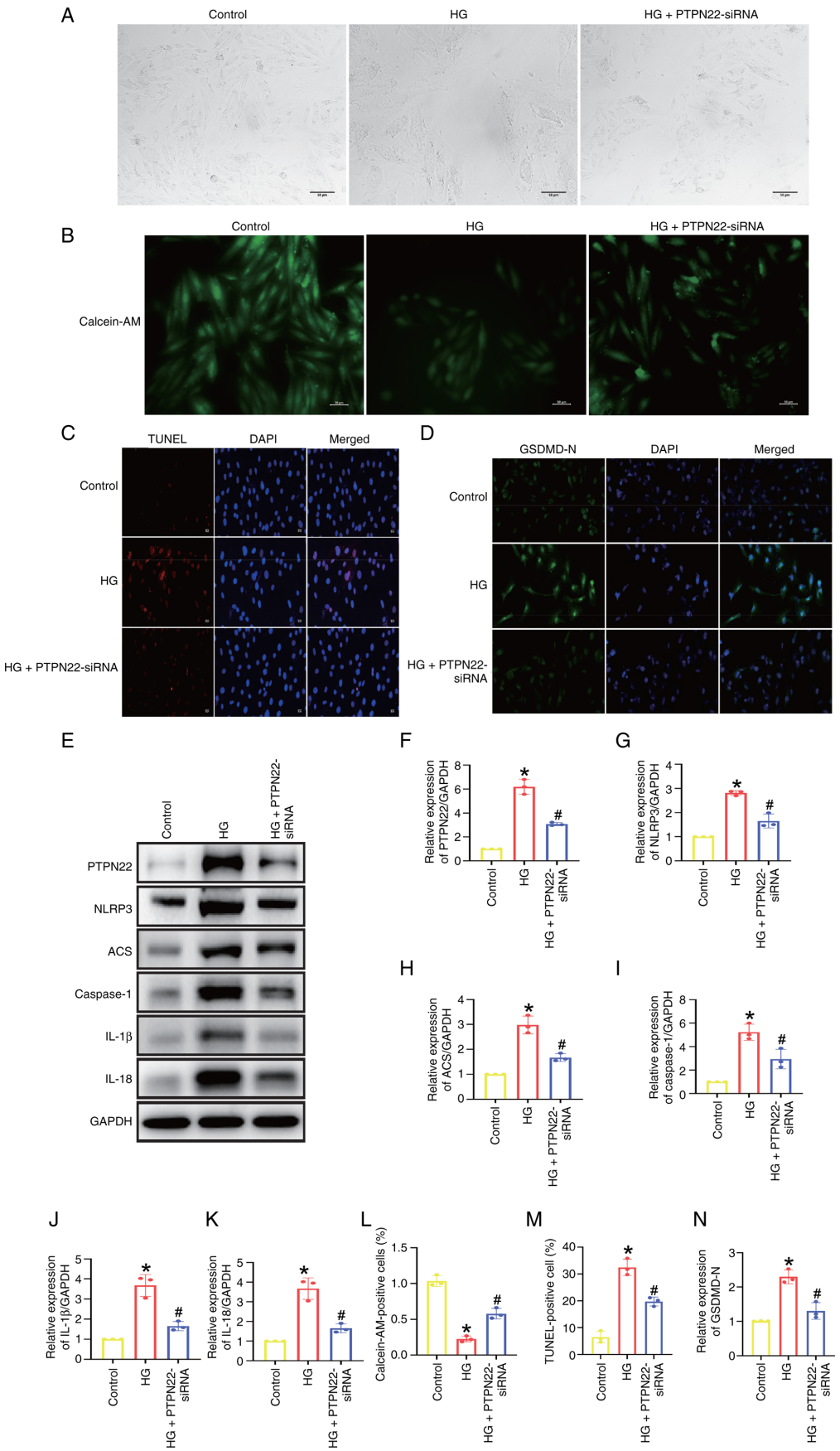

Figure 5. PTPN22 inhibition attenuates HG-induced pyroptosis in H9c2 cells. H9c2 cells were treated with HG or PTPN22-siRNA for 6 h following 48 h incubation in normal culture medium. (A) Morphological changes of H9c2 cells. Scale bar, 50 μm. (B) Calcein-AM, (C) TUNEL and (D) GSDMD-N immunofluorescence staining of H9c2 cells. Scale bar, 20 μm. (E) Western blot analysis of (F) PTPN22, (G) NLRP3, (H) ASC, (I) caspase, (J) IL-1β and (K) IL-18 expression. Quantitative analysis of (L) Calcein-AM staining, (M) TUNEL-positive cells and (N) GSDMD-N immunofluorescence staining. *P<0.05 vs. control; $^{\#}$P<0.05 vs. HG. HG, high-glucose; GSDM, gasdermin; BL, baicalin low; BH, baicalin low; si, small interfering; PTPN, protein tyrosine phosphatase non-receptor type; ASC, apoptosis-associated speck-like protein containing a CARD.

mechanism of the interaction between PTPN22 and TNF-α remains unknown.

There are several limitations to the present study. The absence of additional databases may limit the scope of target screening. The mechanism of baicalin in the treatment of diabetic cardiomyopathy was not fully identified in the present study, since only two common targets and no significant pathways were found with network pharmacology. Future studies should expand the scope of target prediction by introducing more databases to explore the multi-target therapeutic mechanism of baicalin in treating DCM. Furthermore, the present study was only validated in H9c2 cardiomyocytes; to increase clinical translational value, the physiological significance of the identified targets (PTPN22 and TNF-α) and associated pathways must be evaluated in *in vivo* models. In addition, the lack of a positive control makes it difficult to evaluate the relative efficacy and clinical relevance of baicalin. A positive control group should be included in future *in vitro* and *in vivo* studies to verify the therapeutic effects and clinical potential of baicalin against DCM.

The primary reason for not introducing additional databases in the network pharmacology-based target screening process was to ensure the reliability and consistency of the predicted targets. The present study selected Swiss Target Prediction) for baicalin target prediction, which is commonly used in network pharmacology studies of traditional Chinese medicine monomers and has high target prediction accuracy (47-49). This database covers the main target information of baicalin, including its potential binding proteins and associated signaling molecules, which met the needs of target screening for the present study. In addition, the present study considered homogeneity and avoidance of redundant information between databases. Many existing target prediction databases have overlapping target information and introducing too many additional databases may lead to redundant target screening results, increase the complexity of target intersection analysis and introduce false-positive targets due to differences in database prediction algorithms and data sources. This would not only fail to improve the comprehensiveness of target screening but also affect the accuracy and efficiency of experimental verification. Additionally, the present study used a relatively high cutoff value (>30) for target screening, which decreased the number of targets that were originally screened, which had an impact on the number of common targets. Furthermore, the present study aimed to verify the therapeutic effect and underlying mechanisms of baicalin on DCM through *in vitro* experiments; network pharmacology was used as an auxiliary tool to screen potential targets and guide subsequent experimental design. The *in vitro* results supported the validity of the network pharmacology predictions.

Although KEGG pathway analysis did not reveal any significant enriched pathways, the two identified common targets (PTPN22 and TNF-α) are associated with the pathogenesis of DCM. PTPN22 is associated with myocardial inflammation (50), oxidative stress (51) and cardiomyocyte apoptosis (52), which are key pathological processes of DCM. PTPN22 can regulate the activation of T cells and release of inflammatory factors, thereby participating in the progression of DCM (53). Similarly, TNF-α is a classical pro-inflammatory cytokine that plays a pivotal role in the development of DCM by inducing myocardial inflammation, promoting cardiomyocyte pyroptosis and impairing cardiac function (54). These well-documented associations between the two targets and DCM pathogenesis support their potential as key therapeutic targets of baicalin in DCM (55,56). In addition, the selection of PTPN22 and TNF-α was based on the reliability of network pharmacology prediction results. Although the present study only identified two common targets due to the limitations of database selection and high screening cutoff value, these targets were consistently predicted by the databases. The present study verified the binding ability of baicalin to PTPN22 and TNF-α through molecular docking experiments, which showed strong binding affinity, indicating that baicalin directly bound these two targets and exerted regulatory effects. The molecular docking verification further confirms the rationality of selecting these two targets. Furthermore, considering the multi-target and multi-pathway characteristics of traditional Chinese medicine monomers, the lack of enriched KEGG pathways does not mean that the identified targets are invalid. Traditional Chinese medicine monomers typically exert therapeutic effects by regulating multiple targets and signaling pathway networks, rather than relying on a single or significantly enriched pathways. Here, baicalin inhibited the expression of PTPN22 and TNF-α and suppressed the downstream inflammatory and pyroptosis pathways mediated by these targets. These results not only confirm the regulatory effect of baicalin on the two targets but also explain the potential therapeutic mechanism of baicalin in treating DCM from the perspective of target regulation.

In conclusion, the primary cell response to baicalin was suppression of inflammation and pyroptosis. By regulating the activation of the PTPN22 and TNF-α signaling pathways, baicalin inhibited inflammation and pyroptosis in DCM. TNF-α and PTPN22 were key factors in the development of DCM and PTPN22 was involved in pyroptosis. Therefore, dual targeting of these two pathways may represent a promising strategy for treating DCM by treating HG-induced pyroptosis with baicalin.

Acknowledgements

Not applicable.

Funding

The present study was supported by Science and Technology Plan Project of Wenzhou Municipality (grant no. Y2023414).

Availability of data and materials

The data generated in the present study may be requested from the corresponding author.

Authors' contributions

XZ wrote the manuscript and designed the experiments. LX analyzed data. NZ performed the experiments and edited the manuscript. LX and NZ confirm the authenticity of all the raw data. All authors have read and approved the final manuscript.

Ethics approval and consent to participate

Not applicable.

Patient consent for publication

Not applicable.

Competing interests

The authors declare that they have no competing interests.

References

1. Xie SY, Liu SQ, Zhang T, Shi WK, Xing Y, Fang WX, Zhang M, Chen MY, Xu SC, Fan MQ, *et al*: USP28 serves as a key suppressor of mitochondrial morphofunctional defects and cardiac dysfunction in the diabetic heart. Circulation 149: 684-706, 2024.
2. Dillmann WH: Diabetic cardiomyopathy. Circ Res 124: 1160-1162, 2019.
3. Hölscher ME, Bode C and Bugger H: Diabetic cardiomyopathy: Does the type of diabetes matter? Int J Mol Sci 17: 2136, 2016.
4. Sun X, Wang X, He Q, Zhang M, Chu L, Zhao Y, Wu Y, Zhang J, Han X, Chu X, *et al*: Investigation of the ameliorative effects of baicalin against arsenic trioxide-induced cardiac toxicity in mice. Int Immunopharmacol 99: 108024, 2021.
5. Chan E, Liu XX, Guo DJ, Kwan YW, Leung GP, Lee SM and Chan SW: Extract of scutellaria baicalensis georgi root exerts protection against myocardial ischemia-reperfusion injury in rats. Am J Chin Med 39: 693-704, 2011.
6. Guo L, Yang J, Yuan W, Li C, Li H, Yang Y, Xue R and Yan K: Baicalein ameliorated obesity-induced cardiac dysfunction by regulating the mitochondrial unfolded protein response through NRF2 signaling. Phytomedicine 126: 155441, 2024.
7. Xin L, Gao J, Lin H, Qu Y, Shang C, Wang Y, Lu Y and Cui X: Regulatory mechanisms of baicalin in cardiovascular diseases: A review. Front Pharmacol 11: 583200, 2020.
8. Zeng Y, Liao X, Guo Y, Liu F, Bu F, Zhan J, Zhang J, Cai Y and Shen M: Baicalin-peptide supramolecular self-assembled nanofibers effectively inhibit ferroptosis and attenuate doxorubicin-induced cardiotoxicity. J Control Release 366: 838-848, 2024.
9. Wang T, Wang S, Jia X, Li C, Ma X, Tong H, Liu M and Li L: Baicalein alleviates cardiomyocyte death in EAM mice by inhibiting the JAK-STAT1/4 signalling pathway. Phytomedicine 128: 155558, 2024.
10. Hu S, Jiang L, Yan Q, Zhou C, Guo X, Chen T, Ma S, Luo Y, Hu C, Yang F, *et al*: Evidence construction of baicalin for treating myocardial ischemia diseases: A preclinical meta-analysis. Phytomedicine 107: 154476, 2022.
11. Zhao F, Fu L, Yang W, Dong Y, Yang J, Sun S and Hou Y: Cardioprotective effects of baicalein on heart failure via modulation of Ca(2+) handling proteins in vivo and in vitro. Life Sci 145: 213-223, 2016.
12. Luan Y, Sun C, Wang J, Jiang W, Xin Q, Zhang Z and Wang Y: Baicalin attenuates myocardial ischemia-reperfusion injury through Akt/NF-κB pathway. J Cell Biochem 120: 3212-3219, 2019.
13. Yu H, Chen B and Ren Q: Baicalin relieves hypoxia-aroused H9c2 cell apoptosis by activating Nrf2/HO-1-mediated HIF1α/BNIP3 pathway. Artif Cells Nanomed Biotechnol 47: 3657-3663, 2019.
14. Cheng Y, Yan M, He S, Xie Y, Wei L, Xuan B, Shang Z, Wu M, Zheng H, Chen Y, *et al*: Baicalin alleviates angiotensin II-induced cardiomyocyte apoptosis and autophagy and modulates the AMPK/mTOR pathway. J Cell Mol Med 28: e18321, 2024.
15. Nogales C, Mamdouh ZM, List M, Kiel C, Casas AI and Schmidt HHHW: Network pharmacology: Curing causal mechanisms instead of treating symptoms. Trends Pharmacol Sci 43: 136-150, 2022.
16. Zhang P, Zhang D, Zhou W, Wang L, Wang B, Zhang T and Li S: Network pharmacology: Towards the artificial intelligence-based precision traditional Chinese medicine. Brief Bioinform 25: bbad518, 2023.
17. Zhu N, Huang B, Zhu L and Wang Y: Potential mechanisms of triptolide against diabetic cardiomyopathy based on network pharmacology analysis and molecular docking. J Diabetes Res 2021: 9944589, 2021.
18. Denny P, Feuermann M, Hill DP, Lovering RC, Plun-Favreau H and Roncaglia P: Exploring autophagy with gene ontology. Autophagy 14: 419-436, 2018.
19. Zhao X, Huang B, Zhang J, Xiang W and Zhu N: Celastrol attenuates streptozotocin-induced diabetic cardiomyopathy in mice by inhibiting the ACE / Ang II / AGTR1 signaling pathway. Diabetol Metab Syndr 15: 186, 2023.
20. Livak KJ and Schmittgen TD: Analysis of relative gene expression data using real-time quantitative PCR and the 2(-delta delta C(T)) method. Methods 25: 402-408, 2001.
21. Tan Y, Zhang Z, Zheng C, Wintergerst KA, Keller BB and Cai L: Mechanisms of diabetic cardiomyopathy and potential therapeutic strategies: Preclinical and clinical evidence. Nat Rev Cardiol 17: 585-607, 2020.
22. Ritchie RH and Abel ED: Basic mechanisms of diabetic heart disease. Circ Res 126: 1501-1525, 2020.
23. Gulsin GS, Swarbrick DJ, Hunt WH, Levelt E, Graham-Brown MPM, Parke KS, Wormleighton JV, Lai FY, Yates T, Wilmot EG, *et al*: Relation of aortic stiffness to left ventricular remodeling in younger adults with type 2 diabetes. Diabetes 67: 1395-1400, 2018.
24. Nichols GA, Gullion CM, Koro CE, Ephross SA and Brown JB: The incidence of congestive heart failure in type 2 diabetes: An update. Diabetes Care 27: 1879-1884, 2004.
25. Thrainsdottir IS, Aspelund T, Thorgeirsson G, Gudnason V, Hardarson T, Malmberg K, Sigurdsson G and Rydén L: The association between glucose abnormalities and heart failure in the population-based Reykjavik study. Diabetes Care 28: 612-616, 2005.
26. Aksnes TA, Kjeldsen SE, Rostrup M, Omvik P, Hua TA and Julius S: Impact of new-onset diabetes mellitus on cardiac outcomes in the valsartan antihypertensive long-term use evaluation (VALUE) trial population. Hypertension 50: 467-473, 2007.
27. Ohkuma T, Komorita Y, Peters SAE and Woodward M: Diabetes as a risk factor for heart failure in women and men: A systematic review and meta-analysis of 47 cohorts including 12 million individuals. Diabetologia 62: 1550-1560, 2019.
28. Zhang P, Wu H, Lou H, Zhou J, Hao J, Lin H, Hu S, Zhong Z, Yang J, Guo H and Chi J: Baicalin attenuates diabetic cardiomyopathy in vivo and in vitro by inhibiting autophagy and cell death through SENP1/SIRT3 signaling pathway activation. Antioxid Redox Signal 42: 53-76, 2025.
29. Xu Q, Liu Z, Wang L, Liu G, Zhao L, Yue H and Liu Y: Baicalin protects against myocardial fibrosis through inhibition of DOT1L/COL-1 pathway during diabetic cardiomyopathy. Sci Rep 16: 1914, 2025.
30. Sheng X, Wang J, Guo J, Xu Y, Jiang H, Zheng C, Xu Z, Zhang Y, Che H, Liang S, *et al*: Effects of baicalin on diabetic cardiac autonomic neuropathy mediated by the P2Y12 receptor in rat stellate ganglia. Cell Physiol Biochem 46: 986-998, 2018.
31. Wang W, Han R, Lai L and Zhang X: Unlocking the potential: Baicalin's apoptosis-reducing power and activation of NRF2/P62 for alleviating diabetic cardiomyopathy in rats. Mol Cell Toxicol 21: 183-196, 2024.
32. Luo W, Lin K, Hua J, Han J, Zhang Q, Chen L, Khan ZA, Wu G, Wang Y and Liang G: Schisandrin B attenuates diabetic cardiomyopathy by targeting MyD88 and inhibiting MyD88-dependent inflammation. Adv Sci (Weinh) 9: e2202590, 2022.
33. Chen G, Cao P and Goeddel DV: TNF-induced recruitment and activation of the IKK complex require Cdc37 and Hsp90. Mol Cell 9: 401-410, 2002.
34. Newton K and Dixit VM: Signaling in innate immunity and inflammation. Cold Spring Harb Perspect Biol 4: a006049, 2012.
35. Qian K, Shan L, Shang S, Li T, Wang S, Wei M, Tang B and Xi J: Manganese enhances macrophage defense against mycobacterium tuberculosis via the STING-TNF signaling pathway. Int Immunopharmacol 113: 109471, 2022.
36. Coll RC, Schroder K and Pelegrín P: NLRP3 and pyroptosis blockers for treating inflammatory diseases. Trends Pharmacol Sci 43: 653-668, 2022.
37. Fu Y, Shen J, Li Y, Liu F, Ning B, Zheng Y and Jiang X: Inhibition of the PERK/TXNIP/NLRP3 axis by baicalin reduces NLRP3 inflammasome-mediated pyroptosis in macrophages infected with *mycobacterium tuberculosis*. Mediators Inflamm 2021: 1805147, 2021.
38. Meng L, Lin H, Huang X, Weng J, Peng F and Wu S: METTL14 suppresses pyroptosis and diabetic cardiomyopathy by downregulating TINCR lncRNA. Cell Death Dis 13: 38, 2022.
39. Liu P, Zhang Z, Chen H and Chen Q: Pyroptosis: Mechanisms and links with diabetic cardiomyopathy. Ageing Res Rev 94: 102182, 2024.

40. Zeng C, Duan F, Hu J, Luo B, Huang B, Lou X, Sun X, Li H, Zhang X, Yin S and Tan H: NLRP3 inflammasome-mediated pyroptosis contributes to the pathogenesis of non-ischemic dilated cardiomyopathy. Redox Biol 34: 101523, 2020.
41. Wei Z, Gao R, Sun Z, Yang W, He Q, Wang C, Zhang J, Zhang X, Guo L and Wang S: Baicalin inhibits influenza A (H1N1)-induced pyroptosis of lung alveolar epithelial cells via caspase-3/GSDME pathway. J Med Virol 95: e28790, 2023.
42. Wang X, Wei G, Ding Y, Gui X, Tong H, Xu X, Zhang S, Sun Z, Ju W, Li Y, *et al*: Protein tyrosine phosphatase PTPN22 negatively modulates platelet function and thrombus formation. Blood 140: 1038-1051, 2022.
43. Spalinger MR, Lang S, Gottier C, Dai X, Rawlings DJ, Chan AC, Rogler G and Scharl M: PTPN22 regulates NLRP3-mediated IL1B secretion in an autophagy-dependent manner. Autophagy 13: 1590-1601, 2017.
44. Chang HH, Ho CH, Tomita B, Silva AA, Sparks JA, Karlson EW, Rao DA, Lee YC and Ho IC: Utilizing a PTPN22 gene signature to predict response to targeted therapies in rheumatoid arthritis. J Autoimmun 101: 121-130, 2019.
45. Shaw AM, Qasem A and Naser SA: Modulation of *PTPN2/22* function by spermidine in CRISPR-Cas9-edited T-cells associated with crohn's disease and rheumatoid arthritis. Int J Mol Sci 22: 8883, 2021.
46. Ghorban K, Ezzeddini R, Eslami M, Yousefi B, Sadighi Moghaddam B, Tahoori MT, Dadmanesh M and Salek Farrokhi A: PTPN22 1858 C/T polymorphism is associated with alteration of cytokine profiles as a potential pathogenic mechanism in rheumatoid arthritis. Immunol Lett 216: 106-113, 2019.
47. Cao F, Guo C and Guo J: Deciphering CSU pathogenesis: Network toxicologyand molecular dynamics of DOTP exposure. Ecotoxicol Environ Saf 291: 117864, 2025.
48. Shang L, Wang Y, Li J, Zhou F, Xiao K, Liu Y, Zhang M, Wang S and Yang S: Mechanism of Sijunzi Decoction in the treatment of colorectal cancer based on network pharmacology and experimental validation. J Ethnopharmacol 302: 115876, 2023.
49. Gong W, Sun P, Li X, Wang X, Zhang X, Cui H and Yang J: Investigating the molecular mechanisms of resveratrol in treating cardiometabolic multimorbidity: A network pharmacology and bioinformatics approach with molecular docking validation. Nutrients 16: 2488, 2024.
50. Bottini N and Peterson EJ: Tyrosine phosphatase PTPN22: Multifunctional regulator of immune signaling, development, and disease. Annu Rev Immunol 32: 83-119, 2014.
51. Buczyńska A, Sidorkiewicz I, Hryniewicka J, Zbucka-Krętowska M, Dzięcioł J, Szelachowska M and Krętowski AJ: Pregnancy-associated thyroid disorders: The role of genetic, epigenetic, and oxidative stress factors. Rev Endocr Metab Disord 26: 679-692, 2025.
52. Negro R, Gobessi S, Longo PG, He Y, Zhang ZY, Laurenti L and Efremov DG: Overexpression of the autoimmunity-associated phosphatase PTPN22 promotes survival of antigen-stimulated CLL cells by selectively activating AKT. Blood 119: 6278-6287, 2012.
53. Zhang K, Li Y, Ge X, Meng L, Kong J and Meng X: Regulatory T cells protect against diabetic cardiomyopathy in db/db mice. J Diabetes Investig 15: 1191-1201, 2024.
54. Elmadbouh I and Singla DK: BMP-7 attenuates inflammation-induced pyroptosis and improves cardiac repair in diabetic cardiomyopathy. Cells 10: 2640, 2021.
55. Fang T, Wang J, Sun S, Deng X, Xue M, Han F, Sun B and Chen L: JinLiDa granules alleviates cardiac hypertrophy and inflammation in diabetic cardiomyopathy by regulating TP53. Phytomedicine 130: 155659, 2024.
56. Liang H, Yang S, Huang Y, Zhu Y, Wu Q, Wu Z, Li S, Shi Y, Chen Z, Jin H and Wang X: PTPN22 as a therapeutic target in intervertebral disc degeneration: Modulating mitophagy and pyroptosis through the PI3K/AKT/mTOR axis. J Adv Res 80: 775-789, 2026.